Localization and Road Boundary Recognition in Urban Environments Using Digital Street Maps

Kiyoshi Irie and Masahiro Tomono

***Abstract*— In this study, we aim to achieve autonomous navigation for robots in environments that they have not previously visited. Many of the existing methods for autonomous navigation require a map to be built beforehand, typically by manually navigating the robot. Navigation without maps, i.e., without any prior information about the environment, is very difficult. We propose to use existing digital street maps for autonomous navigation. Nowadays digital street maps (e.g., those provided by Google Maps) are widely available and used routinely. Reuse of existing maps for robots eliminates extra cost of building maps. One of the difficulties in using existing street maps is data association between a robot's observation and the map, because the physical entities that correspond to the boundary lines in the map are unknown. We address this issue by using region annotations such as roads and buildings and prior knowledge. We introduce a probabilistic framework that simultaneously estimates a robot's position and the road's boundaries. We evaluated our method in complex urban environments. Our method successfully localized in environments that includes both roadways and pedestrian walkways.**

Fig. 1. Examples of road boundaries in urban environments. Various boundaries such as walls, curbs, guard rails and color differences are shown. Some of the boundaries have no height differences (bottom three images); hence they can not be found by curb-like obstacle detection.

I. INTRODUCTION

Outdoor navigation by mobile robots has been studied extensively. However, navigation in urban environments including pedestrian walkways is still a challenge.

Existing methods for mobile robot navigation can be categorized into two types: map based and recognition based. In the first approach, a robot localizes itself on the map. Although many methods using this approach have been proposed, they require manual navigation of the robot to construct a map. In addition, the cost of building a large-area map is high. Moreover, robots cannot navigate in environments that they have not previously visited. As an example of the recognition-based approach, a robot navigates by finding and tracking the road that leads to its destination given as a GPS coordinate. Although this approach attempts navigation in unseen environments, robust road recognition in real-world situations is still difficult.

As an intermediate approach, we propose to use existing digital street maps for mobile robot localization. Reuse of existing street maps eliminates the extra cost of map construction. Another advantage is that existing maps provide prior information of the environment being mapped. This information can drastically reduce the difficulty of road boundary recognition.

A significant problem in localization using existing maps is the difficulty of associating the boundary lines shown in the maps with sensor observations. Existing map-based localization assumes that the relationship between a map's contents and physical entities is known (e.g., lines on the map denote lane markings). However, street maps are drawn for human use. Hence, the physical entities that are represented by the boundary lines are not explicitly mentioned in the map; a line can denote any type of boundary such as a wall or a curb. This makes it difficult to correlate data between observations and the map. Although Hentschel et al. proposed to use street maps for navigation [1], their localization method uses only building information in the map which can be easily matched with laser scanner observations.

We address this issue by introducing a probabilistic framework that simultaneously estimates the position of the robot and the road boundaries. The key aspect of our method is the use of region annotations on the map and prior knowledge of the environment. Some of the existing digital street maps contain region information such as roads and buildings, in addition to boundary lines. Combining this annotation and the knowledge that people have (e.g., at boundaries between a sidewalk and a roadway, curbs are more often used than walls), we can use prior information to predict the physical entity that corresponds to the boundary line on a map.

Map errors create another difficulty for street map-based localization. Street maps are typically created by hand using aerial photography and are often inaccurate. We address these errors in a probabilistic manner. Error handling methods are integrated into our framework.

The main contributions of this paper are as follows:

- Development of a probabilistic framework for simultaneous localization and road boundary recognition utilizing prior information.

Kiyoshi Irie and Masahiro Tomono are with Future Robotics Technology Center, Chiba Institute of Technology, 2-17-1 Tsudanuma, Narashino-shi, Chiba , Japan {irie, tomono}@furo.org

- Integration of map error handling methods into our framework.

Our proposed method introduces the possibility of navigation in places that a robot has not visited before. We verified the effectiveness of our method through a series of experiments in a challenging real-world environment.

II. RELATED WORK

Many methods for autonomous navigation have been studied. Most of the proposed methods can be categorized into two types: map based and recognition based. Some of the recent studies in the first category include methods using a LIDAR intensity map [2], a landmark map [3], and an image sequence map [4]. In these methods, maps are built from manually collected sensor data.

Recognition-based navigation does not require a detailed map. Instead, robots navigate toward their destinations by finding and tracking the road. Extensive research has been conducted on road detection and tracking. Methods of road detection using a vision system [5], a laser scanner [6], and probabilistic road boundary tracking [7] [8] have been proposed. In the DARPA Urban Challenge, autonomous vehicle navigation with a recognition-based approach was achieved [9]. However, Levinson and Thrun pointed out that navigation in real urban environments is more difficult than in the environment used in the challenge [2]. In particular, pedestrian walkways are more complex than the roadways; for example, sometimes road edges are not as apparent as roadways (Fig. 1). Additionally, GPS is not always reliable in pedestrian walkways because of multipath problems.

Digital maps have been employed for localization in the ITS research community. Mueller et al. proposed a topological localization method on the basis of crossroad detection [10]. Mattern et al. employed a detailed lane markings map and a camera [11]. Hentschel et al. employed building information in publicly available street maps and a laser scanner [1]. In these methods, the correspondence between landmarks in the map (lane markings and walls) and observations was apparent. However, the data association problem between various kinds of boundaries and observations has been left unaddressed.

Regarding use of prior information, several authors employed aerial photography for SLAM. Früh and Zakhor used detected edges in aerial photography for 2D laser-based localization [12]. One of the challenges in using aerial photography is data association. Kümmerle et al. used a 3D laser scanner to make the data association robust to occlusions [13]. Parsley and Julier addressed the difficulty of data association between the edge map and sensor readings [14] . They used latent structures to utilize high-level features for data associations between different types of maps. Our data association problem is similar to this; a significant difference is that we use additional prior information: region information and human knowledge. Those methods above focus on map construction, not navigation. Hence, road boundary recognition, which is an important aspect of online navigation is not achieved by these methods.

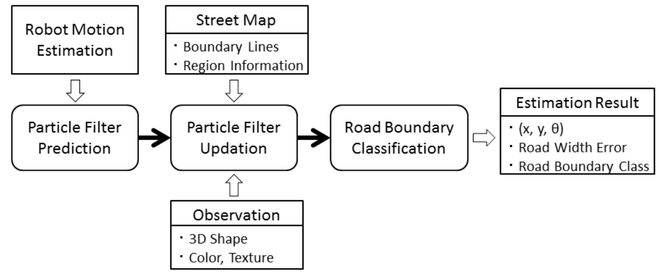

Fig. 2. System Overview.

The advantages of the digital street maps over aerial photography are that these maps do not rely on image processing, road regions and boundaries are clearly given, and annotations are provided by humans, which can be useful beyond localization (e.g., path planning). Although maps for human use are usually less accurate than aerial photography, our map error handing mechanism compensates for this disadvantage.

III. OUR APPROACH

Our approach is outlined in this section.

i. Use of existing maps intended for humans

Our method uses an existing digital street map that contains region information. We assume that the regions in the map are fully annotated. We use three types of annotations: *roadway*, *sidewalk* and *building*.

ii. Human knowledge as prior information

Human knowledge is used as prior information to make recognition easier. For example, if a high wall is found along a sidewalk, it is more likely to be a boundary between the sidewalk and a building rather than the boundary of a roadway. Using both the map and this knowledge, we can make assumptions for object recognition. Thus, the problem becomes far easier than the generic object recognition problem.

iii. Simultaneous estimation of position and road boundary

Some of the probabilistic methods are known to be effective for mobile robot localization [15] [16]. We construct a probabilistic framework for simultaneous localization and road boundary classification on the basis of the Monte Carlo Localization [15]. The prior information is represented in a probabilistic form and used in the framework.

iv. Map error handling

Existing maps for humans often contain errors, leading to failure of localization. We model errors such as small misalignments, road widths, and block lengths in a probabilistic manner to address the errors within the framework mentioned above.

IV. PROPOSED METHOD

Fig. 2 shows the overview of our method. We use a digital street map that contains boundary and region information.

TABLE I

INPUT MAP LABELS $\mathcal{M}$

Category	Labels
Region	Road
	Sidewalk
	Building and everything else
Boundary	Road-Sidewalk
	Sidewalk-Building
	Building-Road

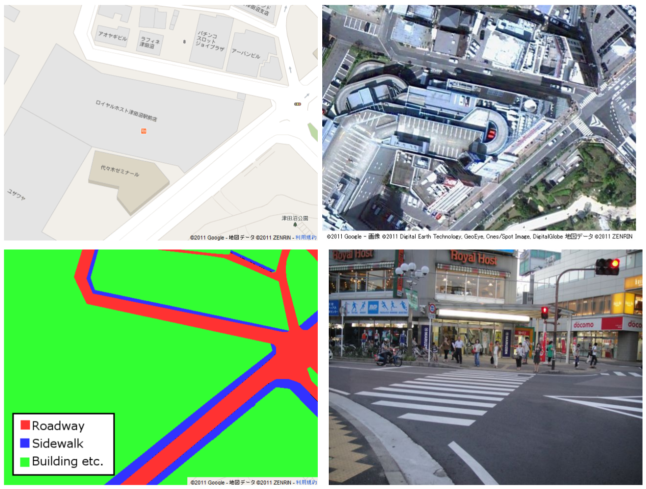

Fig. 3. Top-left: an example of an existing street map. Top-right: aerial photography. Bottom-left: region annotations we use in our methods are shown by colors. Bottom-right: an image taken in the environment.

Our localization uses a particle filter; the essence of our method lies in the updating step in which the position of the robot, road width error and road boundary classes are simulaneously estimated.

A. Map Representation

We use an existing digital street map containing region information and boundaries. In our method, we assume that (at least) three types of region annotations: *sidewalk*, *roadway* and *building*, are provided in the map. Note that the annotation *building* includes buildings and everything except roadways and pedestrian ways. We use an existing street map in the form of 2D grid map. Each cell in the grid map has one of the labels shown in Table. I. We refer to the grid map representation of an existing street map as the *global grid map*. Converting existing maps into global grid maps is out of the scope of this work. In the experiments described in this paper, we used manually generated grid maps. An example of an existing street map and the annotations we use are shown in Fig. 3.

B. Localization

Our localization method uses a particle filter on the basis of Monte Carlo Localization [15]. The robot is assumed to navigate on a flat surface and the 2D pose (position and orientation) of the robot, $\boldsymbol{x} = (x, y, \theta)$, is estimated. In this paper we focus on the position tracking problem when the initial pose of the robot is given. In the prediction step of the particle filter, we draw a new generation of the particle set using a motion model. In the update step, we use a local 2D grid map that contains cues to find road boundaries. We refer to the grid map as the *observation grid map*. In our current implementation, the grid map contains 3D shape, colors and edges detected by a stereo camera (see section V for details). Since our framework does not rely on specific sensor type, other sensors such as a laser scanner can be used as well.

When the robot's motion estimation is given, we predict the pose of the robot. For each particle, we draw a new generation of a particle $\boldsymbol{s}_t^i$, according to the probability of the robot pose given the previous state $\boldsymbol{s}_{t-1}^i$ and relative movement of the robot $\Delta \boldsymbol{x}_t$.

$$\boldsymbol{s}_t^i \sim P(\boldsymbol{x}_t | \boldsymbol{x}_{t-1} = \boldsymbol{s}_{t-1}^i, \Delta \boldsymbol{x}_t). \tag{1}$$

In the update step, a local observation grid map $Z = \{z_1, ..., z_n\}$ is generated. We denote a cell of the observation grid map by z_j. The particles are resampled according to the weight proportional to the likelihood of Z given $\boldsymbol{s}^i$ and global grid map M

$$\omega^i \propto P(Z | \boldsymbol{s}^i, M). \tag{2}$$

We approximate the likelihood of the observation by the product of cell-wise likelihood by

$$P(Z | \boldsymbol{s}^i, M) \approx \prod_j P(z_j | m_k)^{\alpha}, \tag{3}$$

assuming the independence between grid map cells. Where k is the coordinate on the global map that corresponds to z_j when the robot pose is $\boldsymbol{s}^i$. $m_k \in \mathcal{M}$ is the map label at k. Since grid cells are not really independent each other, $\alpha (< 1)$ is used to weaken the independence assumption [17]. Here, we face the data association problem. Calculating eq. (3) directly is not easy because the relationship between the map label m_k and the sensor readings z_j is unclear.

To break down the large problem into smaller pieces, we introduce a hidden variable $r \in \mathcal{R}$ that represents a road boundary class. Classes used in our method are shown in Table. II. We denote the road boundary class at k by r_k. By using r, eq. (3) can be expanded as

$$P(z_j | m_k) = \sum_{r_k \in \mathcal{R}} P(z_j | r_k, m_k) P(r_k | m_k). \tag{4}$$

Making the approximation $P(z_j | r_k, m_k) \approx P(z_j | r_k)$, we calculate cell-wise likelihood as follows.

$$P(z_j | m_k) = \sum_{r_k \in \mathcal{R}} P(z_j | r_k) P(r_k | m_k). \tag{5}$$

This derivation was inspired by [18]. Now eq. (3) is decompose into two easier likelihood calculations. The first part $P(z_j | r_k)$ is the observation likelihood given the boundary type, which is far easier than eq. (3) because relationship between the observation and the boundary type is apparent. The second half $P(r_k | m_k)$ represents the likelihood of road boundary type given the map label, which can be given using the prior knowledge on the environment (i.e. a curb is more likely than a wall on the boundary between a sidewalk and a roadway).

TABLE II

ROAD BOUNDARY CLASSES $\mathcal{R}$

Class	Description
Wall	Vertical flat surface
Curb	Curb and small step
Line	Line, Color change
Plants	Bush, tree
Guard rail	Rail, bars
Not a boundary	Road, sidewalk, building

C. Road Boundary Classification

If the robot pose is known, the correspondence between a cell in the observation grid map z and a cell in the global grid map m can be uniquely determined and the road boundary class of the global grid map cell can be estimated as

$$\hat{r} = \underset{r \in \mathcal{R}}{\operatorname{argmax}} P(r|z,m). \quad (6)$$

Using Bayes theorem, we obtain

$$\begin{aligned} P(r|z,m) &\propto P(z|r,m)P(r|m) \\ &\approx P(z|r)P(r|m). \quad (7) \end{aligned}$$

We consider estimation of road boundary classes when robot pose is given as a probability distribution. We again denote the correspondence between the observation grid map and the global grid map, in terms of robot pose x, by z_j and m_k. The probability that global map cell at k belongs to the class r_k given Z and M is calculated

$$\begin{aligned} P(r_k|Z,M) &\approx \int_x P(r_k|z_j,m_k)dx \\ &\propto \int_x P(z_j|r_k)P(r_k|m_k)dx. \quad (8) \end{aligned}$$

Since we have the distribution of the robot pose as a set of particles, the integral can be calculated by summing up particle-wise likelihood as

$$\hat{r}_k = \underset{r \in \mathcal{R}}{\operatorname{argmax}} P(r_k|Z,M) \quad (9)$$

$$P(r_k|Z,M) \propto \sum_{\boldsymbol{s}^i} P(z_j|r_k)P(r_k|m_k). \quad (10)$$

Since the term $P(z_j|r_k)P(r_k|m_k)$ is identical as eq. (5), we can reuse the intermediate calculation results of the observation likelihood. Thus, we have the robot pose estimation and the road boundary classification simultaneously.

D. Handling Map Errors

Existing street maps often contain errors. There are various kinds of errors, such as small misalignments and incorrect road widths. In our experiences, relatively large errors are often found in the width of roads and the length of blocks. In this section we present error handling methods integrated within our localization framework.

1) Minor Map Errors: To handle small misalignments in maps, we introduce a probabilistic map. Each cell in the map has a set of probabilities that the "true" label of the cell is $m \in \mathcal{M}$. So far we assume that the distance of misalignments (x_ε and y_ε in the map coordinates) follows a normal distribution. The probability that the "true" label of the map cell at $k = (x, y)$ is m' can be calculated as

$$P_k(m') = \int\int \delta_{m'}(x + x_\varepsilon, y + y_\varepsilon)G(x_\varepsilon, y_\varepsilon)dx_\varepsilon dy_\varepsilon. \quad (11)$$

Here $G(x, y)$ is a 2-dimentional Gaussian function and $\delta_{m'}(x, y)$ is a function that returns 1 when the "original" map label at the location is m', otherwise returns 0. This can be easily implemented as the Gaussian filtering.

Using this error model, eq. (3) is rewritten as

$$P(Z|\boldsymbol{s}^i, M) \approx \prod_j \{\sum_{m'} \sum_r P(z_j|r_k)P(r_k|m')P_k(m')\}^\alpha. \quad (12)$$

2) Road Width Estimation: We propose a road width estimation method integrated within the localization framework. Our approach is similar to probabilistic lane tracking methods [7] [8]. We estimate the error ratio d between true road width w' and road width in the map w that satisfies $w = dw'$. Adding d to the state vector, $\boldsymbol{x} = (x, y, \theta, d)$ is estimated by the framework described in section IV-B. Our assumption on the road width is that the width depends on the street blocks and the width changes gradually within a street block.

We give the initial value of d as a uniform distribution from [0.5:2.0]. As the robot moves a certain distance, we predict d as follows.

$$d_t = d_{t-1} + N(0, \sigma_d^2) \quad (13)$$

The standard deviation σ_d^2 is determined empirically. In the update step of the localization, we do not directly observe d; instead, we scale the observation grid map laterally using d in matching it with the global grid map. When robot arrives at the end of a street block, the distribution of d is re-initialized by the uniform distribution.

3) Handling Length Errors: The length of a street block is also often incorrect. When robot is navigating along a street, large error is found at an intersection. This problem can be considered as a kind of kidnapped robot problem [19] [20] [21]. We address the issue by continuously adding random particles that distribute in the longitudinal direction, taking into account the length error.

V. IMPLEMENTATION

A. Sensor

We describe our current implementation used in the experiments in this paper. The only sensor used is a stereo camera. We obtain 3D point clouds and camera motion estimation using edge point based stereo SLAM presented by Tomono [22]. The advantage of using a stereo camera is that we can obtain both 3D information and color and texture information at high frame rates. The disadvantages are the limited field of view and range distance.

TABLE III

FEATURES USED FOR OBSERVATION

Category	Feature	Dimensions
3D info	shape	4
Color	H from HSI	15
	S from HSI	15
Textures and Edges	Edge strength	8
	Edge length	5
	Valley/step edges	5

B. Motion Estimation

In the prediction step of the particle filter, we use a motion model using the camera motion estimation obtained by the stereo SLAM [22]. The 3D camera motion is projected onto the 2D surface as described in [23], to obtain robot motion estimation.

C. Generation of Observation Grid Maps

Each cell in our observation grid map consists of a set of histograms containing 3D features, colors, textures and edges. List of features are summarized in Table. III. An observation grid map is generated as follows. First, a 3D point cloud obtained by the stereo SLAM is stored in a 3D grid map. Second, for each cell in the 3D grid map, 3D shape, color and edges are detected and stored into the cell. Finally, a 2D observation grid map is generated by summarizing the 3D grid map into the 2D grid map.

1) 3D information: The 3D shape is detected by the distribution of 3D points including 26-neighbor cells. A 3D cell is given one from the following labels: *wall*, *vertical bar*, *horizontal bar* and *others*.

2) Color, Texture and Edge: Color, texture and edge properties are detected in the images by projecting the 3D grid cell onto the image. We use HSI color space; H and S values are quantized and stored into 15-dimentional histograms. Edges are detected by canny filter [24]. The strength, the length and the intensity changes of an edge (whether it is a valley or a step edge) are also quantized, counted and stored in the histograms. These features are useful to detect road boundaries without 3D features such as lines, color differences and texture differences.

D. Calculation of Observation Likelihood

To calculate the observation likelihood, we calculate cell-wise observation likelihood by a product of feature-wise observation likelihood. Denoting features stored in an observation grid cell z by $f_1, ...f_N$,

$$P(z|r) \approx \prod_i P(f_i|r). \tag{14}$$

We train $P(f_i|r)$ using labeled data sets.

E. Maps

Our ultimate goal is a system that can handle an existing digital street map without any pre-processing by human; however, we have not implemented the feature yet. So far we annotate maps by hand. We use a captured image of Google Map, and annotations are given by colors. See Fig. 3 for an example.

Fig. 4. Device used in experiments

Fig. 5. Images used in the first experiment.

The prior information, $P(r_l|m_l)$ in eq. (5), is given manualy, based on how often each type of road boundary is found in the environment. Table. IV shows an example of likelihood given as the prior information.

VI. EXPERIMENTS

We carried out experiments in environments close to Tsudanuma station. We collected image sequences using a PointGrey Bumblebee2 stereo camera, mounted on a wheelchair (Fig. 4). Experiments are executed off-line. The size of the images used was 640×480.

The observation likelihood $P(f_i|r)$ is learnt from 21,708 images that were not used for the localization experiments. The size of the global and observation grid map cell was 23.5cm, which is the same as the distance per pixel of the map we used.

A. Localization and Road Classification in a Sidewalk

The result of the position tracking in a 150m sidewalk course is shown in Fig. 6. The reference trajectory drawn by hand is also shown. Our proposed method successfully tracked the path without significant errors; we consider the localization result to be sufficiently accurate for navigation tasks [1].

The processing time measured on a desktop PC with Core i7 3.47GHz was approximately 90ms for each prediction step, and 300ms for each update step. The number of particles employed was 100.

During the position tracking, 653 map cells were classified as road boundaries. We compared the result with the ground

[1]A quantitative evaluation of the localization accuracy is difficult because the map contains errors, and there is no ”exact correspondence” between a location in the map and the world.

TABLE IV
EXAMPLE OF PROBABILITIES USED AS PRIOR KNOWLEGE $P(r|m)$.

		Road boundary class (r)					
		Not a boundary	Line	Curb	Wall	Guard rail	Plants
Map (m)	Roadway-Sidewalk boundary	0.02	0.23	0.35	0.05	0.25	0.1
	Sidewalk-Building boundary	0.02	0.3	0.13	0.3	0.05	0.2
	Building-Roadway boundary	0.02	0.28	0.15	0.35	0.1	0.1

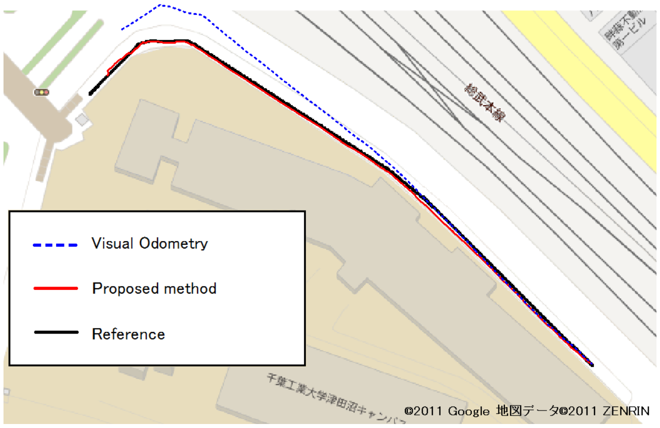

Fig. 6. Position tracking result of the first experiment. Reference trajectory is drawn by hand.

		Estimated Label			
		Curb	Wall	Guard rail	Plants
Truth	Curb	68	0	13	0
	Wall	0	503	0	7
	Guard rail	0	0	36	0
	Plants	16	0	10	0

Fig. 7. The confusion matrix of road boundary classification.

truth generated by hand. The confusion matrix is shown in Fig. 7. The overall precision was 93%; while walls on the left side of the course were classified well, some of the curbs at the right side were missing. This is because edges of the curbs were not apparent and they are sometimes occluded by trees (see Fig. 5 left image). The classification results on plants were not good because of poor illumination conditions (Fig. 5 right). Incorporating different sensor observations such as laser scanners would improve the result.

B. Position Tracking in a Challenging Urban Environment

We evaluated our method in a more complex environment. We collected images in a crowded residential street where there are apartment buildings, stores, parking lots, and a hospital. The challenging route includes both sidewalks and roadways, and there are several apparent errors in road widths and lengths. We compared the performance of the proposed method with and without our map error handling mechanism.

The result and images used are shown in Fig. 8. Our proposed method successfully kept track of the robot pose without catastrophic errors. The method without map error handlings, on the other hand, had significant localization errors. At point C, both methods had a relatively large error because of ambiguous road boundaries.

The road width estimation is evaluated in four sidewalks in the course (Fig. 8 A, B, E, I). The widths of these sidewalks are all incorrect in the map; the differences between the width in the map and the actual width are 0.6m to 1.3m. The results are summarized in Fig. 9. At three points (A, B, I), our method successfully estimated the road width with the accuracy of 0.3m. However, at point E, the estimation was wrong. As seen in Fig. 8, two candidates of the boundary are found at right side of the robot. Since the road width is incorrect, we lack information to solve the data association and the map error estimation simultaneously.

VII. CONCLUSIONS

In this paper, we proposed a new localization and road boundary recognition method using an existing digital street map. Use of existing maps eliminates the cost of map construction. A significant challenge in this approach was to make correct association between the map and the observations. We used annotations on the map and prior knowledge to solve this problem. A framework is constructed that simultaneously localizes the robot and classifies the road boundaries. We also proposed a map error handling mechanism that is integrated within the framework. We conducted experiments in real-world urban environments. We have demonstrated that the digital street map-based localization is possible despite several map errors.

REFERENCES

[1] M. Hentschel and B. Wagner, "Autonomous robot navigation based on OpenStreetMap geodata," in *Proc. of the IEEE Int. Conf. on Intelligent Transportation Systems (ITSC)*, 2010, pp. 1645–1650.

[2] J. Levinson and S. Thrun, "Robust vehicle localization in urban environments using probabilistic maps," in *Proc. of the IEEE Int. Conf. on Robotics & Automation (ICRA)*, 2010, pp. 4372–4378.

[3] Y. M. Saiki, E. Takeuchi, A. Carballo, W. Tokunaga, H. Kuniyoshi, A. Aburadani, A. Hirosawa, Y. Nagasaka, Y. Suzuki, and T. Tsubouchi, "1km autonomous robot navigation on outdoor pedestrian paths "running the Tsukuba challenge 2007"," in *Proc. of the IEEE Int. Conf. on Intelligent Robots & Systems (IROS)*, 2008, pp. 219–225.

[4] H. Katsura, J. Miura, M. Hild, and Y. Shirai, "A view-based outdoor navigation using object recognition robust to changes of weather and seasons," in *Proc. of the IEEE Int. Conf. on Intelligent Robots & Systems (IROS)*, vol. 3, oct. 2003, pp. 2974–2979.

[5] J. Crisman and C. Thorpe, "SCARF: a color vision system that tracks roads and intersections," *IEEE Trans. on Robotics and Automation*, vol. 9, no. 1, pp. 49–58, 1993.

[6] T. Saitoh and Y. Kuroda, "Online road surface analysis using laser remission value in urban environments," in *Proc. of IROS*, 2010, pp. 15–21.

[7] R. Danescu and S. Nedevschi, "Probabilistic lane tracking in difficult road scenarios using stereovision," *IEEE Trans. on Intelligent Transportation Systems*, vol. 10, no. 2, pp. 272–282, 2009.

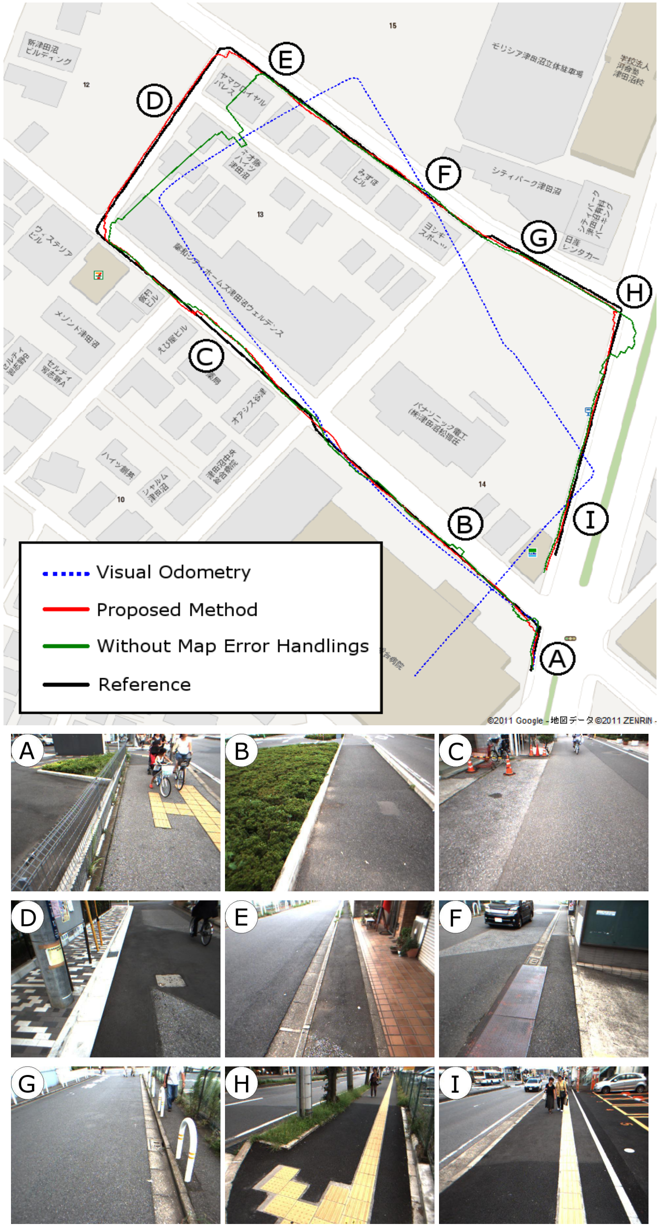

Fig. 8. Result of the second experiment and images used in the experiment.

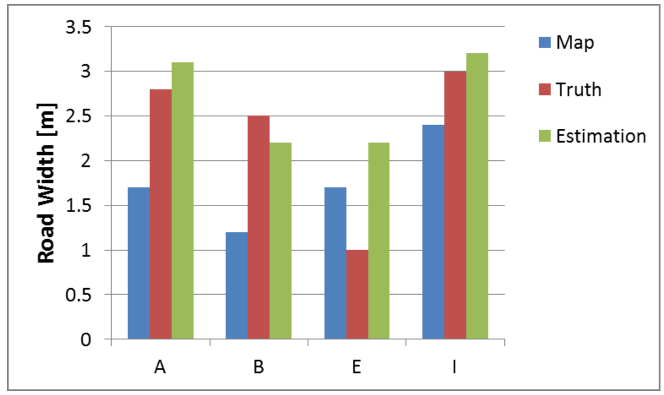

Fig. 9. Result of road width estimation

[8] Y. Matsushita and J. Miura, "Simultaneous estimation of road region and ego-motion with multiple road models," in *IEEE International Conference on Multisensor Fusion and Integration for Intelligent Systems 2008*, 2008, pp. 526–532.

[9] M. Montemerlo, J. Becker, S. Bhat, H. Dahlkamp, D. Dolgov, S. Ettinger, D. Haehnel, T. Hilden, G. Hoffmann, B. Huhnke, D. Johnston, S. Klumpp, D. Langer, A. Levandowski, J. Levinson, J. Marcil, D. Orenstein, J. Paefgen, I. Penny, A. Petrovskaya, M. Pflueger, G. Stanek, D. Stavens, A. Vogt, and S. Thrun, "Junior: The stanford entry in the urban challenge," *J. of Field Robotics*, vol. 25, no. 9, pp. 569–597, 2008.

[10] A. Mueller, M. Himmelsbach, T. Luettel, F. v. Hundelshausen, and H.-J. Wuensche, "GIS-based topological robot localization through lidar crossroad detection," in *Proc. of the IEEE Int. Conf. on Intelligent Transportation Systems (ITSC)*, 2011, pp. 2001–2008.

[11] N. Mattern, R. Schubert, and G. Wanielik, "High-accurate vehicle localization using digital maps and coherency images," in *Proc. of the IEEE Int. Conf. on Intelligent Vehicles Symposium*, 2010, pp. 462–469.

[12] C. Früh and A. Zakhor, "An automated method for large-scale, ground-based city model acquisition," *Int. J. of Computer Vision*, vol. 60, pp. 5–24, 2004.

[13] R. Kümmerle, B. Steder, C. Dornhege, A. Kleiner, G. Grisetti, and W. Burgard, "Large scale graph-based SLAM using aerial images as prior information," *J. of Autonomous Robots*, vol. 30, pp. 25–39, 2011.

[14] M. Parsley and S. Julier, "Towards the exploitation of prior information in SLAM," in *Proc. of the IEEE Int. Conf. on Intelligent Robots & Systems (IROS)*, 2010, pp. 2991–2996.

[15] F. Dellaert, D. Fox, W. Burgard, and S. Thrun, "Monte carlo localization for mobile robots," in *Proc. of the IEEE Int. Conf. on Robotics & Automation (ICRA)*, 1999, pp. 1322–1328.

[16] J. Leonard and H. Durrant-Whyte, "Mobile robot localization by tracking geometric beacons," *IEEE Trans. on Robotics and Automation*, vol. 7, no. 3, pp. 376–382, 1991.

[17] S. Thrun, W. Burgard, and D. Fox, *Probabilistic Robotics*. MIT Press, 2005.

[18] M. Cummins and P. Newman, "FAB-MAP: Probabilistic localization and mapping in the space of appearance," *The Int. J. of Robotics Research*, vol. 6, no. 27, pp. 647–665, 2008.

[19] S. Thrun, D. Fox, W. Burgard, and F. Dellaert, "Robust monte carlo localization for mobile robots," *Artificial Intelligence*, vol. 128, no. 1-2, pp. 99–141, 2000.

[20] S. Lenser and M. Veloso, "Sensor resetting localization for poorly modelled mobile robots," in *Proc. of the IEEE Int. Conf. on Robotics & Automation (ICRA)*, vol. 2, 2000, pp. 1225–1232.

[21] R. Ueda, T. Arai, K. Sakamoto, T. Kikuchi, and S. Kamiya, "Expansion resetting for recovery from fatal error in monte carlo localization - comparison with sensor resetting methods," in *Proc. of the IEEE Int. Conf. on Intelligent Robots & Systems (IROS)*, vol. 3, 2004, pp. 2481–2486.

[22] M. Tomono, "Robust 3D SLAM with a stereo camera based on an edge-point ICP algorithm," in *Proc. of the IEEE Int. Conf. on Robotics & Automation (ICRA)*, 2009, pp. 4306–4311.

[23] K. Irie, T. Yoshida, and M. Tomono, "Mobile robot localization using stereo vision in outdoor environments under various illumination conditions," in *Proc. of the IEEE Int. Conf. on Intelligent Robots & Systems (IROS)*, 2010, pp. 5175–5181.

[24] J. Canny, "A computational approach to edge detection," *IEEE Trans. on Pattern Analysis & Machine Intelligence*, vol. 8, no. 6, pp. 679–698, 1986.